Cellular Microbiology (2008) **10**(7), 1559–1571
doi:10.1111/j.1462-5822.2008.01150.x
First published online 10 April 2008

Bipolar spindle frequency and genome content are inversely regulated by the activity of two N-type kinesins in *Entamoeba histolytica*

Promita Ghosh Dastidar and Anuradha Lohia*
Department of Biochemistry, Bose Institute, Kolkata, India.

Summary

Bipolar microtubular spindles are seen infrequently in *Entamoeba histolytica* trophozoites while monopolar or radial microtubular assemblies are common. Additionally, heterogeneity in nuclear DNA content and multi-nucleation is found in amoeba cells growing in axenic culture. Taken together these observations indicate that genome segregation is irregular in these cells. In order to identify proteins involved in regulating genome segregation, we have focused on studying *E. histolytica* homologues of kinesin motor proteins that are known to affect stability of bipolar mitotic spindles. We have demonstrated earlier that increased levels of the kinesin – Eh Klp5 – led to increased frequency of bipolar spindles accompanied with a reduction in the heterogeneity of genome content, showing that bipolar spindle frequency was inversely linked to genome content in *E. histolytica*. In this study, we have investigated the role of *E. histolytica* kinesins (Eh KlpA1, 2–4) in regulating bipolar spindle frequency and genome content. While downregulation of Eh Klp3, 4 and A1 showed no effect, downregulation of Eh Klp2 led to increased frequency of bipolar spindles and homogenization of genome content, similar to the effect of increased expression of Eh Klp5. In addition to microtubules, Eh Klp2–4 associated with F-actin in the cytoplasm, suggesting that these kinesins are multi-functional.

Introduction

The division of a single cell to generate two daughter cells containing identical genetic material is necessary for proliferation. This process involves genome duplication followed by segregation. In eukaryotes, faithful segregation of chromosomes is accomplished on the bipolar microtubular spindle. In fact, failure to form a bipolar spindle leads to inhibition of genome segregation in all eukaryotes. In the protist pathogen *Entamoeba histolytica*, bipolar microtubular spindles are infrequent while radial microtubular assemblies are commonly visible (Orozco *et al.*, 1988; Vayssie *et al.*, 2004). Recently, Dastidar *et al.* (2007) demonstrated the presence of bipolar spindles in 8–10% of cells only, after taxol treatment. Analysis of the *E. histolytica* cell cycle after serum starvation and re-addition in axenic culture showed a unimodal distribution of cells with heterogenous amounts of DNA and consequently the absence of discrete populations of cells in G1 or G2 phases (Gangopadhyay *et al.*, 1997; Das and Lohia, 2002). This heterogeneity has been ascribed both to genome re-duplication and inefficient genome segregation (Lohia *et al.*, 2007). The study by Dastidar *et al.* (2007) further showed that increased expression levels of the kinesin protein, Eh Klp5, led to an increase in the number of bipolar spindles. This effect may have been achieved either by stabilizing or facilitating bipolar spindle assembly. Concurrent with an increase in bipolar spindle frequency, the reported heterogeneity of genome content was significantly reduced. These observations indicated that increase in bipolar spindles facilitated efficient genome segregation, so that daughter cells contain equivalent amounts of DNA.

Microtubule organization and stability is modulated by the activity of microtubule (MT)-associated proteins and motor proteins of the kinesin and dynein families (Wittman *et al.*, 2001). Kinesin superfamily proteins (also named as KRPs, Klps or KIFs) are defined by the presence of a well-conserved globular domain – the catalytic core or the 'head' that contains both an ATP binding/hydrolysis site (P loop, Switch-I and Switch-II regions) and MT binding sites (Ogawa *et al.*, 2004). In addition to MT binding, some Klps, like GhKCH1, isolated from cotton fibre cells and CHO1 proteins belonging to the mitotic kinesin-like protein 1 subfamily, have been shown to interact directly with the actin filaments during the completion of cytokinesis (Kuriyama *et al.*, 2002; Preuss *et al.*, 2004). Thus, kinesins play a role in regulating both chromosome segregation and cytokinesis depending on the cytoskeletal element that they interact with.

Received 19 November, 2007; revised 27 February, 2008; accepted 17 March, 2008. *For correspondence. E-mail amoeba@boseinst.ernet.in; Tel. (+91) 33 2355 0256; Fax (+91) 33 2355 3886.

Phylogenetically, kinesins are classified into 14 different subfamilies based on the conserved features of their motor domains, because the 'stalk/tail' region is highly divergent even within the members of a single family (Miki *et al*., 2005). Of the 14 subfamilies, kinesin-1, 2, 3 and 9 family members are involved in organelle transport and Kinesin-5, 6, 7, 10, 13 family members take part in mitosis – specifically in regulating microtubular spindle assembly and function (Miki *et al*., 2005; Wickstead and Gull, 2006). Members of kinesin-4, 8, 12 and 14 subfamilies can perform multiple functions, including chromosome segregation, cytokinesis and transport of cargo (Miki *et al*., 2005). The C-terminal kinesin family 14 was further classified into 14A (mitotic kinesins) and 14B (organelle transporters) subfamilies. Thus different kinesin types exist in a single organism to carry out specific functions.

Entamoeba histolytica encodes four N-terminal kinesin proteins (Eh Klp2–5) and two copies of a C-terminal kinesin (Eh KlpA1/A2) (Dastidar *et al*., 2007). Phylogenetic analysis showed that the nearly identical C-terminal kinesins Eh KlpA1 and A2 belonged to the kinesin-14A family, Eh Klp2 and 3 formed an outgroup to the kinesin-12 family, Eh Klp5 belonged to the Kinesin-5 or BimC family while Eh Klp4 did not cluster with any known kinesins (Wickstead and Gull, 2006; Dastidar *et al*., 2007). Thus, in comparison with the many subfamilies of kinesin motors found in higher eukaryotes, *E. histolytica* has a limited repertoire of kinesins, all of which show important differences from their closest sequence homologues.

In this study, we have examined the role of *E. histolytica* kinesins Eh Klp2–4 and A1 in regulating spindle frequency. Our results show that decreased levels of Eh Klp2 affected spindle frequency and concurrently genome content in amoeba, while downregulation of Eh Klp3, 4 and A1 did not show any significant effect on spindle frequency or genome content. We have discovered that in addition to microtubular assemblies, Eh Klp2–4 were also associated with F-actin, suggesting their involvement in actin-associated cellular functions. This study compares the roles of Eh Klp2 with Eh Klp5 in regulating bipolar spindles and genome content in *E. histolytica*.

Results

Conserved domains in E. histolytica *kinesins*

On the basis of homology in the motor domains, we had earlier classified *E. histolytica* kinesins with kinesin-14A (Eh KlpA1/A2), kinesin-5 (Eh Klp5), kinesin-12 (Eh Klp2, 3) while Eh Klp4 was unique (Dastidar *et al*., 2007). In order to better understand the cellular functions of the *E. histolytica* kinesin-like proteins, we have now analysed their primary sequences for conserved functional motifs and domains. Kinesins are multi-domain proteins possessing a globular motor domain for ATP hydrolysis and MT binding, a central coiled coil (CC) region for dimer formation (stalk) and a non-CC domain responsible for light chain interaction and cargo binding (Hirokawa *et al*., 1998; Kim and Endow, 2000). Apart from the characteristic motor, stalk and tail domains, Klps from different organisms also possess other functional regions like leucine zipper (LZ), *trans*-membrane (TM) domain, forkhead homology-associated and pleckstrin homology domains at the non-motor region (Kollmar and Glöckner, 2003; Richardson *et al*., 2006).

Based on the position of their motor domain, Eh Klp2–5 were classified as N-type and Eh KlpA1/A2 as C-type kinesins. All the Eh Klps displayed α helical CC regions outside the motor domain (Fig. 1A). In addition, the DNA binding domain defined by the LZ motif was detected in Eh Klp3 (Fig. 1A). Several conserved features of the kinesin-5 family were identified in Eh Klp5 along with some significant differences. Similar to the members of kinesin-5 family, Eh Klp5 contained the 'fourth coiled coil domain' near the C-terminus which could be required for promoting spindle stability (Hildebrandt *et al*., 2006). However, the BimC box required for association of kinesin-5 proteins with the spindle as observed in Xenopus and human cells (Blangy *et al*., 1995; Sawin and Mitchison, 1995) was absent in Eh Klp5, like the *Saccharomyces cerevisiae* Cin8 and Kip1(Drummond and Hagan, 1998). Additionally, Eh Klp5 contained five KEN boxes that may be targeted by the anaphase-promoting complex (Gordon and Roof, 2001; Hildebrandt and Hoyt, 2001), suggesting that expression of Eh Klp5 may be regulated during the cell cycle.

Eh Klp4 was one of the most divergent kinesin homologues identified yet (Dastidar *et al*., 2007). Domain analysis of Eh Klp4 showed the presence of a TM motif and a short CC region within its motor domain (Fig. 1A). Sequence alignment of Eh Klp4 (Fig. 1B) with human kinesin heavy chain and other Eh Klps showed that several conserved residues involved in ATP binding, hydrolysis and MT binding were absent or altered in Eh Klp4. These amino acids have been shown to be important for motor activity of kinesin molecules (Sablin *et al*., 1996; Dagenbach and Endow, 2004). It is intriguing that in spite of the absence of crucial conserved residues, this protein was recognized as a kinesin homologue by different search engines although it could not be grouped with any known kinesin (Dastidar *et al*., 2007).

In order to verify the functional capacity of the motor domains of Eh Klp2–4 and A1, their motor domains were expressed as recombinant proteins in *Escherichia coli* expression vector and assayed for ATPase activity. All four Eh Klps showed similar ATPase activity in their motor domains (Fig. S1) like Eh Klp5 (Dastidar *et al*., 2007). Although sequence analysis of Eh Klps showed several changes from kinesin homologues, their motor domains showed functional catalytic activity.

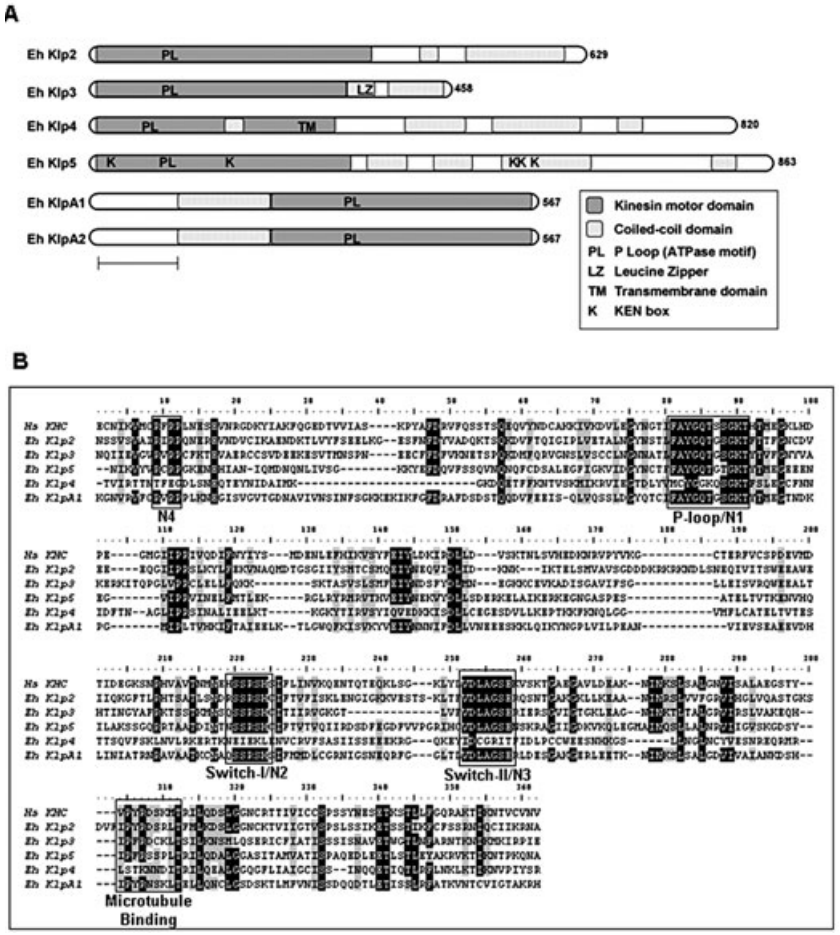

Fig. 1. Conserved domains in *E. histolytica* Kinesins.
A. Identification of conserved domains in *E. histolytica* kinesins. A schematic representation of conserved domains in Eh Klp2–5 and A1 is shown. Conserved sequence motifs have been identified from homology searches in the Pfam domain database (EMBL), Conserved Domain Database (NCBI), SMART, TmPred and 2Zip tools. A key to the domain names and symbols is given in the box. Number of amino acids in each protein is shown on the right. Scale shows 100 amino acids.
B. Multiple sequence alignment of the motor domains of Eh Klps with the human conventional kinesin (Hs KHC). ClustalW alignment of the predicted motor domains from Eh Klp 2–5 and A1 with the motor domain of the human kinesin (Hs KHC) is represented using the BioEdit software. The conserved residues important for ATP hydrolysis (P-loop/N1), ATP binding (Switch-I/N2, Switch-II/N3, N4) and MT interaction (Kull *et al*., 1996; Sablin *et al*., 1996) are shown in boxes. The black- and grey-shaded residues indicate identity and similarity respectively. Dashes indicate gaps introduced for optimal alignment.

Expression of Eh Klp2,3,4 and A1 in E. histolytica

In order to examine the functions of Eh Klp2–4 and A1 in *E. histolytica* trophozoites, CHH [Calmodulin binding domain, hemagglutinin (HA), His] (multi-epitope)-tagged Eh Klps were expressed in stable transformants (as described in Dastidar *et al*., 2007), selected at increasing concentrations of G418 and maintained at 40 μg ml^{-1} G418. Eh Klp2–4 and A1 showed increased RNA (Fig. 2A) and protein (Fig. 2D) expression levels in stable transformants compared with control. Loss of function was studied in stable transformants expressing double-stranded (ds)RNA constructs as described earlier (Dastidar *et al*., 2007). Downregulation of Eh Klp2 and 3 mRNA was around 40–50%, while Eh KlpA1 mRNA was downregulated around 80% compared with control (Fig. 2B). Eh Klp4 dsRNA transformants also showed 40–50% mRNA expression levels of Eh Klp4, compared with control cells [analysed by semi-quantitative reverse transcriptase-polymerase chain reaction (RT-PCR) (Fig. 2B) and quantitative RT-PCR (qRT-PCR) (Fig. 2C)]. Expression of the kinesin proteins Eh Klp2, 3 and A1 were downregulated in dsRNA transformants (Fig. 2D). Changes in protein expression of Eh Klp4 in different transformants could not be determined because of failure of its polyclonal antibody. Expression of Eh Klp4 in stable transformants was monitored by the tagged HA epitope alone. Expression levels of Eh Klp5 in stable transformants have been shown earlier (Dastidar *et al*., 2007). We visualized Eh Klp2, 3, 5 and A1 transformants stained with the polyclonal antisera specific to individual Klps and anti-HA antibody (Fig. S2). Our results show comparable colocalization of both polyclonal and monoclonal antibodies, confirming that epitope-tagged Eh Klps are expressed like endogenous Eh Klps in stable transformants.

Eh Klp2–4 and A1 localize on the microtubular assembly

Microtubular assemblies were visualized in control and Eh Klp transformants after staining with anti-Eh β tubulin polyclonal antibody. Like the wild-type cells (Dastidar *et al*., 2007), transformants expressing Eh Klp2–4, A1 and empty vector showed both radial and bipolar spindle microtubular assemblies (Fig. 3B). CHH-tagged Eh Klp2–4 and A1 were visualized in stable transformants using monoclonal anti-HA antibody and colocalized on

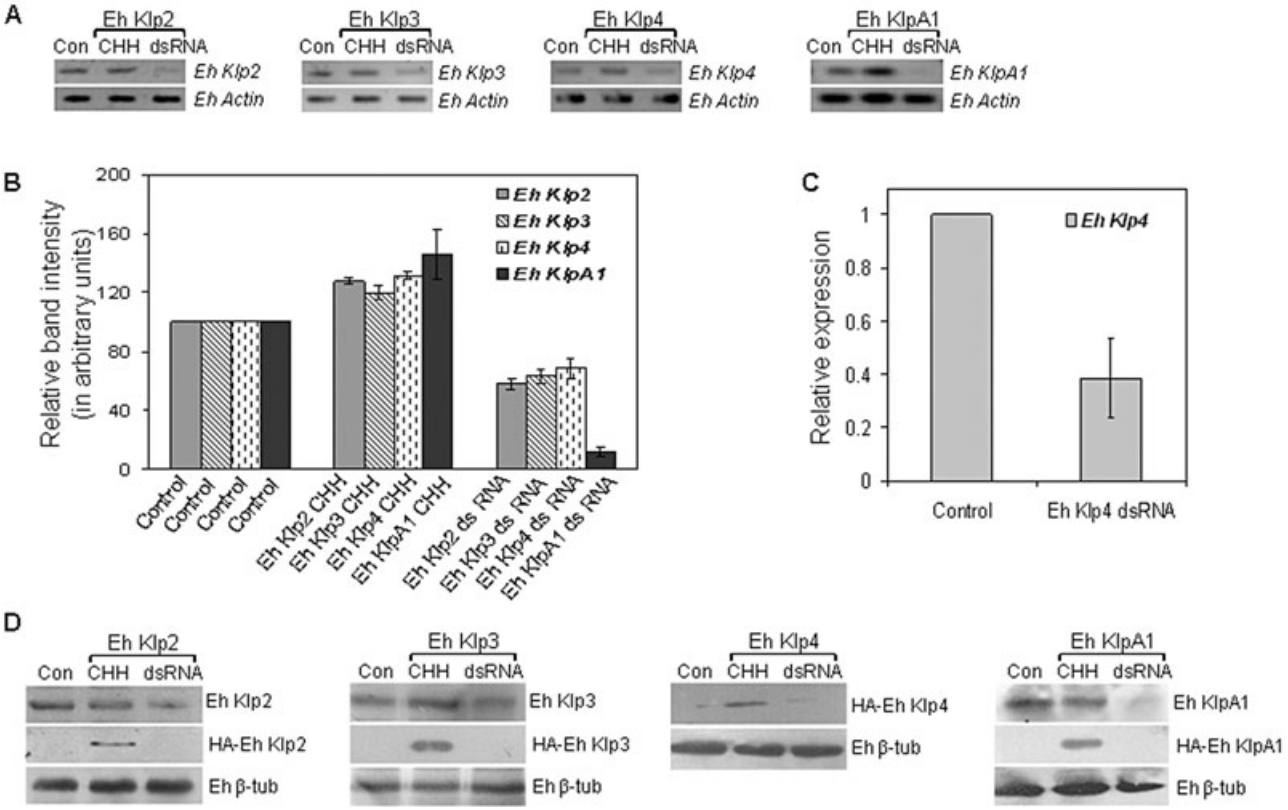

Fig. 2. Expression of Eh Klp2–4 and A1 in stable transformants of *E. histolytica*.
A. RNA from control transformants (Con), CHH multi-epitope-tagged Eh Klp transformants (CHH) and Eh Klp dsRNA transformants (dsRNA) was isolated. Expression of the specific Eh Klp was determined by RT-PCR on equal amounts of RNA, using corresponding primer sets (italics on the right). *Eh Actin* primers were used for endogenous control in all the samples.
B. The gel images (A) were scanned in a densitometer and the relative band intensities of *Eh Actin* and *Eh Klp 2–4* and *A1* RT-PCRs were quantified using Gene tools software (Syngene,USA). Average levels of expression from three independent sets were normalized with respect to *Eh Actin* and represented as a bar diagram. Error bars indicate ± SD ($n = 3$). *X*-axis shows the name of the transformants; *y*-axis shows the relative expression levels of specific kinesins (italicized names represent primers used for expression analysis).
C. Expression of Eh Klp4 in Eh Klp4 dsRNA transformant. qRT-PCR was performed on equal amounts of RNA prepared from control and Eh Klp4 dsRNA transformants (shown on *x*-axis) using *Eh Klp4* primers (inset in bar diagram). *Eh Actin* primers were used for endogenous control. Relative expression of *Eh Klp4* in control and Eh Klp4 dsRNA transformant were plotted as bars. Error bars represent ± SD ($n = 3$).
D. Western blots of cellular proteins from control, CHH epitope-tagged and dsRNA transformants of Eh Klp2–4 and A1 were hybridized with specific polyclonal anti-Eh Klp antisera to detect the expression of Eh Klp2 (~70 kDa), Eh Klp3 (~50 kDa) and Eh KlpA1 (~60 kDa). Monoclonal anti-HA antisera was used to detect the expression of CHH-tagged Eh Klps. Eh β tubulin was used as a loading control in different cell types and detected with the rabbit polyclonal anti-Eh β tubulin antisera.

both MT spindles and radial MTs (Fig. 3A). Eh Klp2, 3 and 4 were also present in the cytoplasm (Fig. 3A).

Polyclonal anti-Eh KlpA1 antibody showed successful downregulation of Eh KlpA1 in dsRNA transformants, although Eh Klp2 and 3 showed low levels of expression in their dsRNA transformants (Fig. S3A). Localization of Eh Klp4 in dsRNA transformants could not be determined because of lack of an anti-Klp4 antibody. Unlike Eh Klp5 dsRNA transformants that showed only radial MTs (Dastidar *et al.*, 2007), bipolar spindle assembly was not inhibited in dsRNA transformants of Eh Klp2–4 and A1 (Fig. S3B).

In order to verify the association with MTs, we isolated proteins bound to Eh Klps by affinity chromatography on Ni-NTA agarose. Our results show that Eh β tubulin was bound to each of the Eh Klps (Fig. 3B). Thus both the microscopy and biochemical experiments confirm the association of Eh Klps with MTs. The MT binding site was predicted by sequence analysis of the motor domains. Although Eh Klp4 sequence showed variations at the MT binding site experimentally both by microscopy and *in vitro* analysis, we show that Eh Klp4 binds MTs.

Eh Klp2, 3 and 4 localize with polymerized F-actin, while Eh Klp5 and A1 do not

Figure 3 showed localization of Eh Klp2–4 both on MT assemblies and in the cytoplasm. As kinesins are also involved in transportation of vesicles and other cellular components, we wondered if these kinesins were bound to the F-actin-based cytoskeleton in the absence of cytoplas-

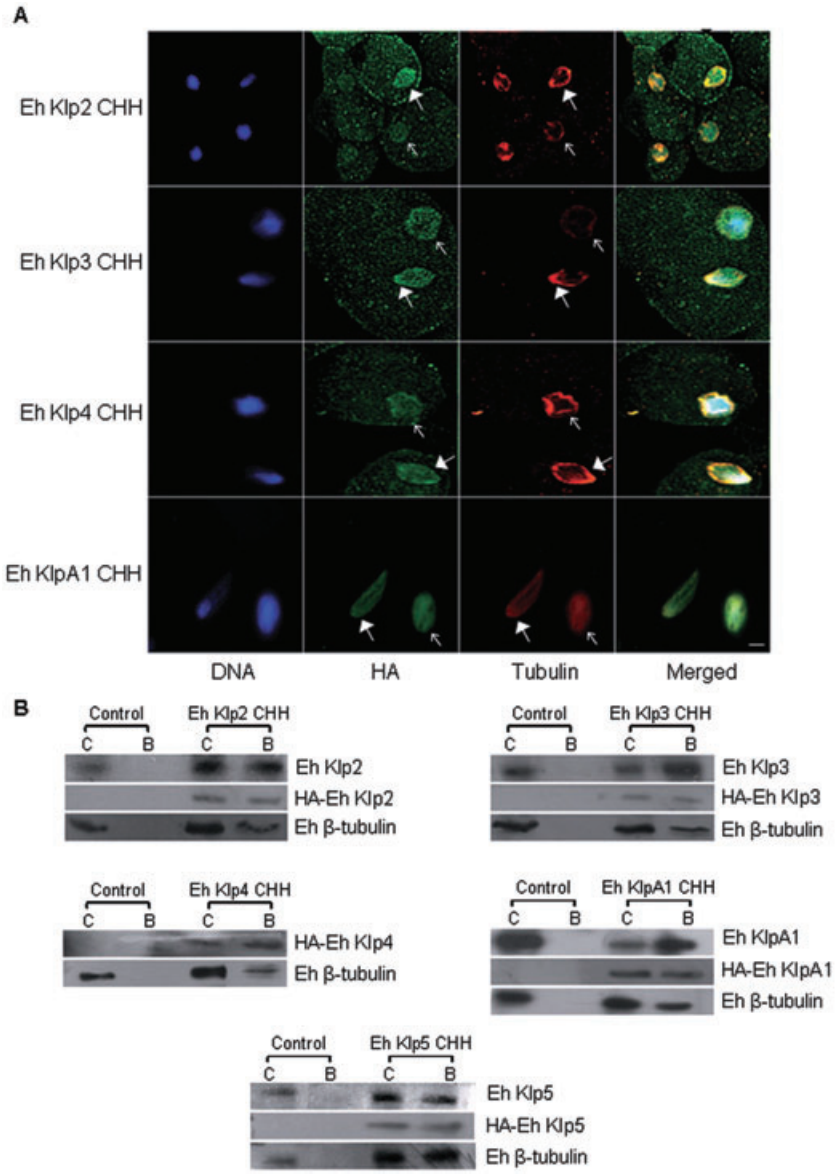

Fig. 3. Eh Klp2–4 and A1 localize on the microtubular assembly.
A. Immuno-localization of Eh Klp2–4 and A1 with tubulin in *E. histolytica*. CHH epitope-tagged Eh Klp2–4 and A1 transformants were stained with mouse monoclonal anti-HA antibody (HA) to detect the corresponding Klp and polyclonal anti-Eh β-tubulin antibody (tubulin). Eh Klp2-CHH, Eh Klp3-CHH, Eh Klp4-CHH and Eh KlpA1-CHH show colocalization with bipolar spindles (white arrows with filled arrow heads) and radial microtubular assemblies (white arrows). DNA was stained with DAPI. Cells were visualized under 40× oil in a Zeiss Axiovert 200 M fluorescence microscope. Bar represents 5 μm.
B. Eh tubulin is bound to Eh Klp2–5 and A1. Cell extracts (C) of Eh Klps CHH transformants and control cells were allowed to bind with Ni-NTA agarose beads (B), and the protein samples were separated by SDS-PAGE followed by Western transfer and hybridization with rabbit polyclonal anti-Eh Klp2, 3, 5 and A1 antibodies, mouse monoclonal anti-HA antibody and polyclonal anti-Eh β tubulin antibody. Tubulin was identified in the beads from Eh Klp CHH transformants, but not in control cells.

mic MTs in *E. histolytica*. Untreated and 10 μM cytochalasin D-treated wild-type *E. histolytica* HM1:IMSS and Eh Klp4 CHH transformant were stained with rabbit polyclonal anti-Eh Klp2, 3, 5 or A1 antibodies or anti-HA antibody (to detect Eh Klp4) and phalloidin. In untreated cells, Eh Klp2, 3 and 4 colocalized with F-actin (Fig. 4A), while Eh Klp5 and A1 showed no association with F-actin and clearly showed spindle-like structures only (Fig. 4A). Treatment of *E. histolytica* cells with cytochalasin D showed loss of F-actin-associated Eh Klp2–4 structures (Fig. 4A), confirming that Eh Klp2–4 were bound to F-actin assemblies.

Association of Eh Klps with actin was verified biochemically by isolation of the actin-rich fraction from the cell lysate (Fig. 4B). Eh Klp2, 3 and 4 were identified in the actin-rich fraction while Eh Klp5 and A1 were not associated. These results suggest that Eh Klp2–4 may participate in cellular functions mediated by the actin cytoskeleton and MT assembly, while Eh Klp5 and A1 appear to be involved in chromosome segregation alone.

Kinesin motor proteins, like GhKCH1 and CHO1, directly interact with F-actin during cell division (Kuriyama *et al*., 2002; Preuss *et al*., 2004). In case of CHO1, a consensus motif for actin binding was not identified in exon 18 (Kuriyama *et al*., 2002). F-actin binding is mediated through the calponin homology domain in KCH1 (Preuss *et al*., 2004) and the C-terminal region of Kin5 (Iwai *et al*., 2004). We compared the sequences of Eh Klp2–4 with the actin binding sites of these kinesins, but a consensus motif could not be identified (data not shown). Although a consensus F-actin binding site could not be identified in Eh Klp2, 3 or 4, we have experimentally demonstrated the binding of Eh Klp2–4 to F-actin by con-

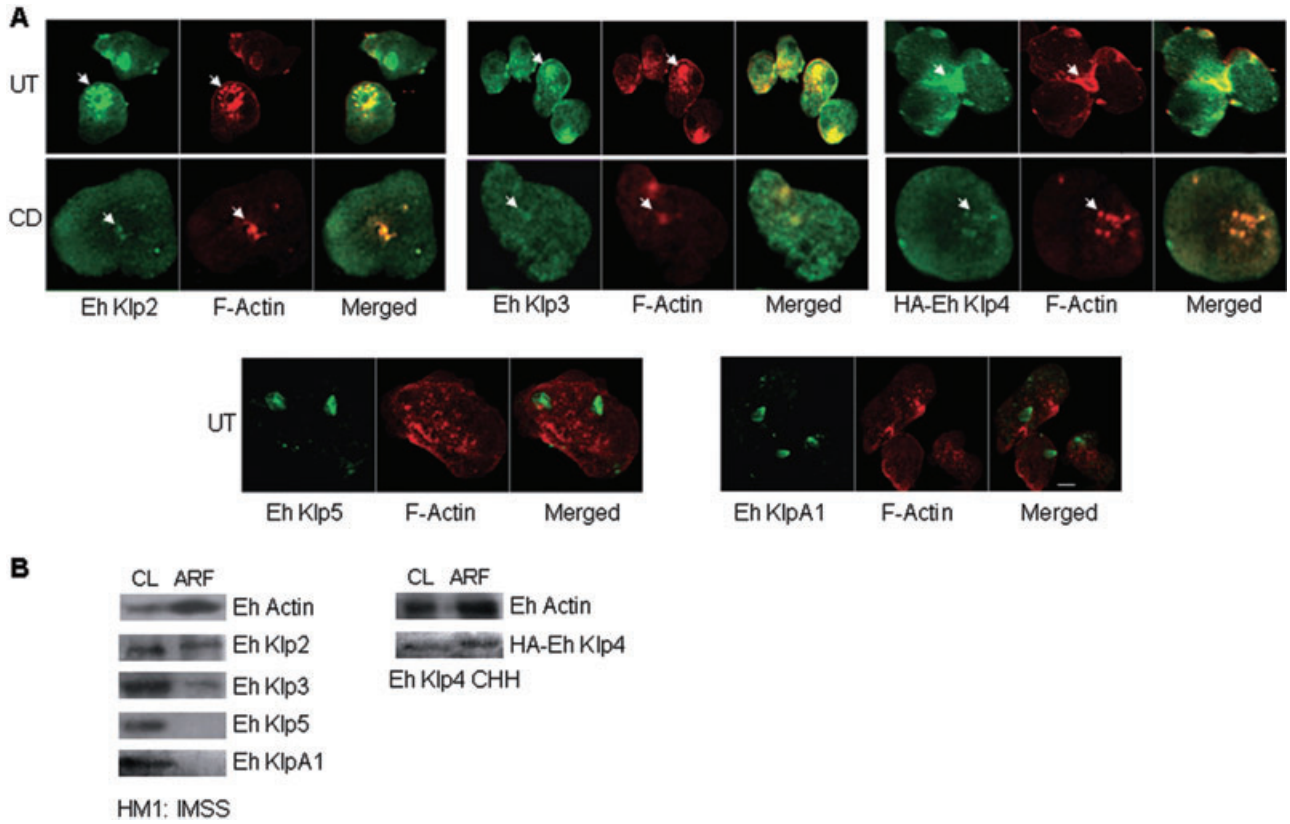

Fig. 4. Eh Klp2–4 localize with polymerized F-actin, while Eh Klp5 and A1 do not.
A. Localization of Eh Klp2–4 with F-actin in untreated and cytochalasin D-treated *E. histolytica* trophozoites. Untreated (UT) and 10 μM cytochalasin D (CD)-treated wild-type *E. histolytica* HM1:IMSS and Eh Klp4 CHH transformant were stained with specific rabbit polyclonal anti-Eh Klp antibody followed by Alexa-Fluor 488-conjugated secondary antibody and rhodamine-conjugated phalloidin. CHH epitope-tagged Eh Klp4 was stained with monoclonal anti-HA antibody and rhodamine-conjugated phalloidin. The localization of Eh Klp2–4-CHH with F-actin was indicated with white arrows in both untreated and cytochalasin D-treated sets. Images were acquired with 63× oil DIC objective in a Zeiss LSM 510 Meta confocal microscope. Bar represents 5 μm.
B. Eh Klp2–4 associate with the actin-rich subcellular fraction while Eh Klp5 and A1 do not. Crude lysates (CL) and actin-rich fraction (ARF) from wild-type *E. histolytica* HM1:IMSS and Eh Klp4 CHH transformant were separated on SDS-PAGE, transferred to Western blots and hybridized with polyclonal Eh Klp2, 3, 5 and A1 antibodies to detect the specific Eh Klps and monoclonal anti-HA antibody to detect CHH-tagged Eh Klp4. Eh Actin was detected with monoclonal anti-β actin antibody in the two sets. Eh Klp2–4-CHH were identified in the actin-rich subcellular fraction while Eh Klp5 and A1 were detected in the crude lysate only.

focal microscopy and *in vitro* association with actin-rich fraction from *E. histolytica* (Fig. 4). Sequence analysis had also suggested the presence of TM domains in Eh Klp4, but microscopy showed that this protein was localized primarily in the cytoplasm.

In the light of our results, it appears that Eh Klp2 , 3, 5 and A1 may associate with MTs directly through their MT binding domains. Binding to polymerized F-actin or monomeric actin may occur directly through undefined actin binding sites or other interacting proteins.

Decreased levels of Eh Klp2 led to an increase in bipolar spindles

Bipolar MT spindles are infrequent in *E. histolytica*, while radial MT assemblies are more common. Our earlier study showed abolition of MT spindles in dsRNA transformants of Eh Klp5 while the frequency of bipolar spindles doubled in Eh Klp5 CHH-stable transformants when compared with control cells (Dastidar *et al.*, 2007). As all the Eh Klps showed association with MTs, we compared the phenotypic effect of changes in their expression levels on the frequency of bipolar spindles in this study. We had earlier quantified bipolar MT spindle frequency after treatment with taxol alone (Dastidar *et al.*, 2007). As the percentage of cells showing bipolar spindles was low, *E. histolytica* cells may be relatively insensitive to taxol. We have now quantified the frequency of bipolar MT spindles in untreated cells and after treatment with 10 μM taxol for 10 h (Table 1). Our results show that frequency of bipolar spindles increased only marginally after treatment with taxol in all the *E. histolytica* cells. Therefore, we have compared bipolar spindle frequency in different transformants without taxol treatment.

Table 1. Frequency of bipolar spindles in Eh Klp transformants.

E. histolytica transformants	% of bipolar spindles ± SD ($n = 3$)	
	Untreated	Taxol
Control	7.3 ± 0.6	8.3 ± 0.6
Eh Klp5-CHH	14.85 ± 1.5	19.8 ± 2.2
Eh Klp5 dsRNA	2.05 ± 0.2	2.1 ± 0.3
Eh Klp2-CHH	6.4 ± 0.4	6.4 ± 0.4
Eh Klp2 dsRNA	11.8 ± 0.1	13.7 ± 1.3
Eh Klp3-CHH	6.9 ± 0.1	8.6 ± 0.1
Eh Klp3 dsRNA	6.6 ± 0.4	8.7 ± 1.8
Eh Klp4-CHH	7 ± 0.4	7 ± 0.2
Eh Klp4 dsRNA	7.35 ± 0.5	7.5 ± 0.2
Eh KlpA1-CHH	6.8 ± 0.3	7.4 ± 0.2
Eh KlpA1 dsRNA	6.4 ± 0.1	7.2 ± 1.1

Entamoeba histolytica cells were grown on coverslips at 37°C with or without 10 μM taxol for 10 h at 37°C followed by fixation with 3.7% formaldehyde. Percentage of cells with bipolar spindles was calculated after staining with anti-Eh β tubulin antibody. Frequency of bipolar spindles was studied in control and Eh Klp transformants in the presence and absence of taxol. Values represent the average spindle frequency from three independent experiments. Approximately 300 cells were counted for each transformant in every set.

Table 1 shows that bipolar spindle frequency was not altered significantly in Eh Klp2 CHH, Eh Klp3 CHH, Eh Klp3 dsRNA, Eh Klp4 CHH, Eh Klp4 dsRNA, Eh KlpA1 CHH and Eh KlpA1 dsRNA transformants compared with control. Bipolar spindle frequency was increased when Eh Klp2 levels were decreased or Eh Klp5 levels were increased. As shown earlier (Dastidar *et al*., 2007), bipolar spindle numbers were reduced significantly when Eh Klp5 was downregulated. Thus of all the Eh Klps, only Eh Klp2 and 5 appeared to play a role in regulating bipolar spindle frequency. Increase in Eh Klp5 expression leads to increased bipolar spindles and decreased levels of Eh Klp5 led to loss of visible bipolar spindles. Decrease in Eh Klp2 on the other hand led to increased numbers of bipolar spindles in the population. Eh Klp2 therefore appears to act as an inhibitor of spindle stability or assembly.

We have earlier shown that Eh Klp2 expression was similar to control cells in Eh Klp5 dsRNA transformants. We now show that expression of Eh Klp5 was similar in Eh Klp2 dsRNA and control cells and Eh Klp2 expression was unaltered in control and Eh Klp5 CHH transformants (Fig. 5). This data show that expression of Eh Klp5 and 2 are not co-ordinately regulated.

The monastrol analogue, HR22C16 A1, was used on Eh Klp5 and 2 transformants to determine if bipolar spindle assemblies were affected by inhibitors of Eh Klp5 in Eh Klp2 dsRNA transformants. It may be seen from Table 2 that the effect of HR22C16 A1 on control and Eh Klp2 transformants was similar (~50% decrease in spindles), while the effect was more pronounced in Eh Klp5 CHH transformants (~70% decrease in spindles). On the other hand, bipolar spindles were abolished when Eh Klp5 was downregulated in dsRNA transformants. As Eh Klp5 structure is altered in the monastrol binding site, the protein is relatively resistant to the drug and, therefore, complete inhibition may not occur (Dastidar *et al*., 2007).

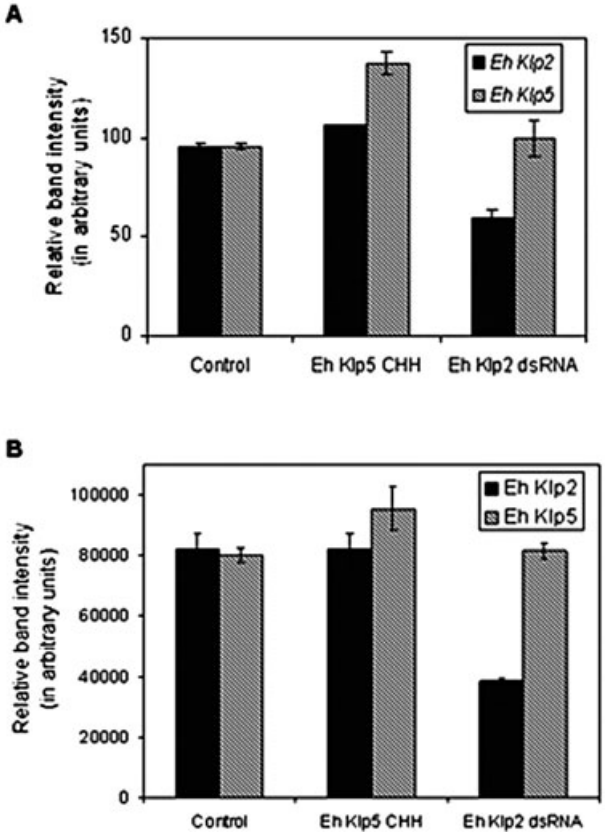

Fig. 5. Expression of Eh Klp2 and 5 in control, Eh Klp5-CHH and Eh Klp2 dsRNA transformants.
A. RT-PCR was carried out on equal amounts of RNA from control, Eh Klp5-CHH and Eh Klp2 dsRNA transformant using *Eh Klp2*, *Klp5* and *actin* primers and analysed by agarose gel electrophoresis. The gel images were scanned in a densitometer and the relative band intensities of Eh Actin, Eh Klp2 and 5 RT-PCRs were quantified using Gene tools software (Syngene,USA). Average levels of expression from three independent sets were normalized with respect to Eh Actin and represented as a bar diagram. Error bars indicate ± SD ($n = 3$). *X*-axis shows the name of the transformants; *y*-axis shows the relative expression levels of specific kinesins (italicized names represent primers used for expression analysis).
B. Western blots of cellular proteins from control, Eh Klp5 CHH and Eh Klp2 dsRNA transformants were hybridized with polyclonal anti-Eh Klp2 antibody, Eh Klp5 antibody and Eh β tubulin antibody. Eh β tubulin was used as a loading control in different cell types. The relative band intensities of Eh β tubulin, Eh Klp2 and 5 expression were quantified using ImageQuant 5.2 software. Average levels of expression from three independent sets were normalized with respect to Eh β tubulin and represented as a bar diagram. Error bars indicate ± SD ($n = 3$). *X*-axis shows the transformants; *y*-axis shows the relative protein expression levels of Eh Klp2 and 5 (names represent antibodies used for expression analysis).

Table 2. Frequency of bipolar spindles in HR22C16 A1-treated Eh Klp5 and 2 transformants.

E. histolytica transformants	% of bipolar spindles ± SD ($n = 3$)	
	Untreated	HR22C16-A1
Control	7.3 ± 0.6	3.5 ± 0.7
Eh Klp5-CHH	14.85 ± 1.5	5.5 ± 0.3
Eh Klp5 dsRNA	2.05 ± 0.2	1.9 ± 0.6
Eh Klp2-CHH	6.4 ± 0.4	3.9 ± 0.1
Eh Klp2 dsRNA	11.8 ± 0.1	7 ± 0.3

Entamoeba histolytica cells were grown on coverslips at 37°C with or without 50 μM HR22C16 A1 for 8 h at 37°C followed by fixation with 3.7% formaldehyde. Percentage of cells with bipolar spindles was calculated after staining with anti-Eh β tubulin antibody. Frequency of bipolar spindles was analysed in control, Eh Klp2 and 5 transformants in the presence or absence of the drug. Values represent the average spindle frequency from three independent experiments. Approximately 300 cells were counted for each transformant in every set.

Taken together, our results suggest that frequency of bipolar spindles was determined by the relative amounts of Eh Klp5 and 2 in a cell. Increase in the ratio of Eh Klp5 to 2 (as seen in Eh Klp5 CHH and Eh Klp2 dsRNA transformants), compared with control cells, led to increased numbers of bipolar spindles. Conversely, decrease in this ratio – as seen in Eh Klp5 dsRNA transformants and *E. histolytica* cells treated with HR22C16 A1 – led to reduced numbers of bipolar spindles.

Downregulation of Eh Klp2 expression reduces the heterogeneity in the genome content of E. histolytica *cells*

Flow cytometric analysis of 48 h cultures showed a reduction in the heterogeneity of genome content in Eh Klp2 dsRNA transformants compared with control and Eh Klp2 CHH transformants (Fig. 6A). It may be noted that the growth rates and cell numbers were the same for all three transformants. Three independent sets were analysed for the distribution of cells with different genome contents. 1×, 2×, 4× and higher genome contents were demarcated by electronic gates (M1–M4) and analysed for the cell numbers (Fig. 6B). The average of three independent experimental sets showed that Eh Klp2 dsRNA transformants contained a significantly higher percentage of cells containing 1× genome content and a reduced population of cells with 4× genome content than Eh Klp2 CHH and control transformants. Thus, decreased expression of Eh Klp2 in Eh Klp2 dsRNA transformants facilitates efficient chromosome segregation possibly as a result of the increased number of bipolar spindles. The same pheno-

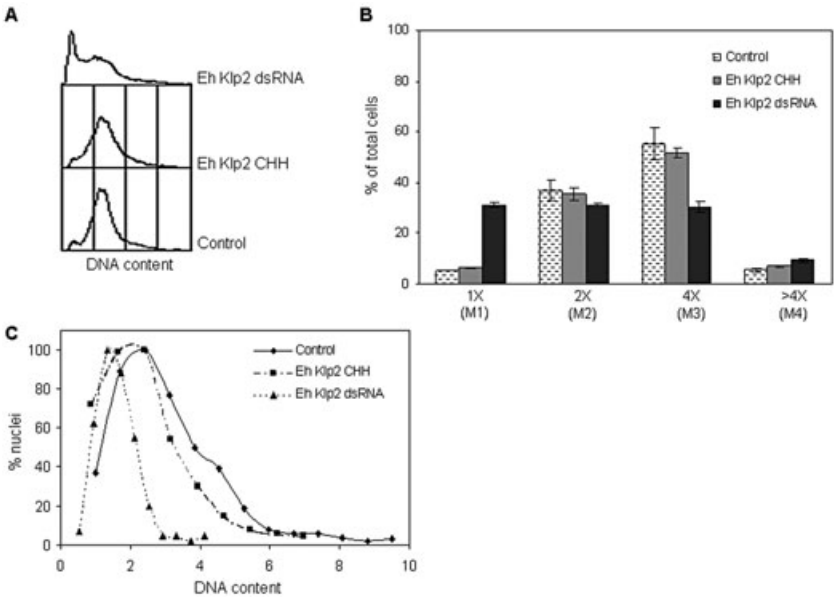

Fig. 6. Effect of Eh Klp2 expression on the genome content of *E. histolytica*.
A. DNA content of 48 h grown control, Eh Klp2-CHH and Eh Klp2 dsRNA transformants analysed by flow cytometry and shown as overlay diagram. *X*-axis shows the DNA content and *y*-axis shows the cell count or number of events. As the histograms are shown as overlay diagrams, the scale could not be shown.
B. Percentage of cells (control, Eh Klp2-CHH and Eh Klp2 dsRNA transformants) in each electronic gate (M1–M4) was estimated from three independent experimental sets. Electronic gates M1–M4 were set to demarcate cells with 1×, 2×, 4× and greater than 4× DNA content respectively. Error bars represent ± SD ($n = 3$).
C. Ethanol-fixed cells of control, Eh Klp2-CHH and Eh Klp2 dsRNA transformants were stained with DAPI and individual nuclei were scanned for DNA content in a MetaCyte scanning cytometer using the software Metafer4. A minimum of 2000 nuclei was scanned for each set. The values were normalized with respect to the empty vector control transformant and represented as histograms.

type was observed earlier (Dastidar *et al*., 2007) in Eh Klp5 CHH transformants when Eh Klp5 levels were increased.

In order to determine if the nuclear genome content was affected by decreased expression of Eh Klp2, we estimated the 4,6-diamidino-2-phenylindole (DAPI) fluorescence (or DNA content) in control and Eh Klp2 transformants. Results obtained from scanning cytometry (Fig. 6C) showed that the average nuclear DNA content of Eh Klp2 dsRNA transformants was significantly lower and more homogeneous than control cells and Eh Klp2 CHH transformants, which showed many nuclei containing more than 4× genome content. Analysis of Eh Klp3, 4 and A1 transformants did not show any appreciable differences in the distribution of average cellular or the nuclear DNA content compared with control cells (Fig. S4). From data presented above and in the earlier paper by Dastidar *et al.* (2007), Eh Klp2 dsRNA transformants and Eh Klp5 CHH transformants show similar reduction of heterogeneity in genome content compared with other transformants and control cells.

Discussion

The activity of the mitotic kinesin motor proteins are required for the assembly of cytoskeletal MTs into a functional bipolar spindle that is essential for segregation of sister chromatids accurately into the two daughter cells. To achieve this function, the spindle appears to progress through a series of dynamic steady state structures that are regulated by a delicate balance of complementary and antagonistic forces generated by the parallel action of multiple mitotic kinesin-like proteins (Sharp *et al*., 2000). Generally, the kinesin-5/BimC family members and the C-type kinesins together function antagonistically to assemble and stabilize the spindle structure through their MT cross-linking and oppositely oriented motor activity (O'Connell *et al*., 1993; Mountain *et al*., 1999).

In *E. histolytica*, expression levels of the kinesin-5/BimC homologue, Eh Klp5 directly affects spindle frequency (Dastidar *et al*., 2007). In this study, we achieved excellent downregulation of the C-type kinesin Eh KlpA, but an associated effect on spindle stability or frequency was not observed. Other studies with C-terminal kinesins have also reported that inhibition of this group of kinesins did not affect the spindle architecture or function *in vivo* (O'Connell *et al*., 1993; Mountain *et al*., 1999).

Partial downregulation of a second N-type kinesin Eh Klp2 increased the number of bipolar spindles in *E. histolytica* while other Eh kinesins had no effect on spindle frequency. Therefore, in addition to the effect of increased expression of Eh Klp5 on bipolar spindle frequency and homogenization of genome content, a second N-type kinesin is now shown to affect spindle frequency and genome content in *E. histolytica*.

Our results indicate that the frequency of bipolar spindles is dependant on the relative amounts of Eh Klp5 and 2 in a cell. Eh Klp2 may regulate the function of Eh Klp5 or spindle assembly directly. At this time, we do not know if this effect is mediated through a common pathway or if Eh Klp2 and 5 act independently. An important distinction in the activity of Eh Klp2 and 5 was observed, where expression levels of Eh Klp5 was directly related to spindle frequency, suggesting that Eh Klp5 was required for spindle assembly or stability. On the other hand, only a decrease in Eh Klp2 levels showed a significant increase in spindle assembly. Thus Eh Klp2 may function as an inhibitor of spindle assembly, where removal of the inhibitor facilitates the formation and stability of bipolar spindles in *E. histolytica.*

In contrast to Eh Klp2 and 5, changes in the expression of the two other N-type kinesins that associated with the MT – Eh Klp3 and 4 – did not show any effect on the spindle assembly or genome content. Phylogenetic analysis based on sequence similarity of kinesin motor domains showed that Eh Klp2 and 3 originated from the same branch (Dastidar *et al*., 2007). However, Eh Klp2 and 3 may bind different substrate molecules through their unique non-motor regions and show differences in subcellular organization. Clearly they performed different functions in the cell, as Eh Klp2 was crucial for determining spindle frequency, unlike Eh Klp3.

The frequency of bipolar spindles affects the genome content of *E. histolytica* cells. Our experiments show that increased spindle frequency correlated with reduced heterogeneity in the genome content of the cell population. Thus genome segregation in *E. histolytica* must occur on bipolar spindles like other eukaryotes. The radial or monopolar assemblies are likely intermediate structures or represent unstable spindles that are incapable of completing genome segregation efficiently.

In conclusion, we have characterized the role of Eh Klp2–5 and A1 in regulating microtubular assemblies in *E. histolytica*. We have also identified three N-terminal kinesins that bind F-actin in addition to MTs. Our results indicate that perturbation of Eh Klp2 or 5 levels alters the frequency of bipolar spindles and genome content in *E. histolytica*. Thus a delicate balance of these two kinesins regulates genome segregation and content in *E. histolytica*, possibly through independent mechanisms. Determining these mechanisms would require identification of proteins interacting with Eh Klp2 and 5 in future.

Experimental procedures

Cell culture and maintenance

Entamoeba histolytica HM1:IMSS trophozoites were maintained axenically in TYIS 33 medium at 37°C (Diamond *et al*., 1978). Cells were routinely subcultured and trophozoites in log phase of

growth (24–48 h) were used in all experiments. Stable transformants were maintained in a similar medium with 40 μg ml^{-1} G418.

Cloning and sequencing of genes encoding E. histolytica *kinesin-like proteins*

Oligonucleotide primers specific for genes encoding *E. histolytica* kinesin-like proteins (designed from the genome sequence of *E. histolytica*, TIGR database) were used in PCR reactions to isolate the *Eh Klps* from genomic DNA, subsequently cloned into pBlueScript SK(-) plasmid and sequenced by automated DNA sequencing (Applied Biosystems, USA). The GenBank Accession Numbers of *E. histolytica* kinesin-like proteins are XP_651474 (Eh KlpA1), XP_651294 (Eh KlpA2), XP_656748 (Eh Klp2), XP_649467 (Eh Klp3), XP_649327 (Eh Klp4) and XP_649446 (EhKlp5). The cDNA sequences of Eh Klp2 and 3 were confirmed by automated DNA sequencing.

Constructs for expressing epitope-tagged Eh Klp and Eh Klp dsRNA

The DNA fragment encoding the multi-affinity epitope tag CHH (Honey *et al*., 2001) was cloned in frame with the 3′ end of *Eh Klp2–4* and *Eh KlpA1* gene in pBS SK(-) and checked by DNA sequencing. *CHH*-tagged *Eh Klps* were individually subcloned in the *E. histolytica* expression vector pJST4 (Ghosh *et al*., 1996) for transformation and expression in *E. histolytica* trophozoites. dsRNA constructs of Eh Klp2–4 and A1 were made as described in Dastidar *et al.* (2007). Three hundred and forty base pairs from the 5′ end (nucleotides 1–340) of the *Eh KlpA1*, 687 bp from the 3′ end (nucleotides 1278–1965) of the *Eh Klp2*, 351 bp from the 3′ end (nucleotides 1075–1426) of the *Eh Klp3* and 400 bp from the 3′ end (nucleotides 2060–2460) of the *Eh Klp4* gene were subcloned in a head-to-head orientation individually, with an intervening λ DNA stuffer (560 bp) fragment in pBS SK(-) vector. Each cassette was cloned under the actin promoter in pJST4 and transformed in *E. histolytica* HM1:IMSS trophozoites. Stable transformants were selected at increasing concentrations of G418 and stably maintained in presence of 40 μg ml^{-1} G418. For the empty vector control, Eh Klp5 CHH and Eh Klp5 dsRNA transformants, we used the constructs described in Dastidar *et al.* (2007).

Raising polyclonal antisera to Eh Klp2, 3 and A1

The 3′ end of *Eh Klp2* (nucleotides 1278–1965), 3′ end of *Eh Klp3* (nucleotides 1075–1426) and 5′ end of *Eh KlpA1* (nucleotides 1–340) were subcloned separately in pJC40 and expressed in *E. coli* BL21 (DE3) as 10× His-tagged proteins. The recombinant proteins were purified and injected into rabbits for raising polyclonal antisera. Rabbit polyclonal antisera were purified on Protein A-agarose beads (Bangalore Genei, India). A similar strategy was used for raising antisera against Eh Klp4, but the antisera did not show specificity and could not be used.

Isolation of RNA from E. histolytica *and RT-PCR*

Total RNA were isolated from the empty vector-transformed control cells, CHH and dsRNA transformants of Eh Klp2–4 and A1 using Trizol reagent (Invitrogen, USA). Semi-quantitative RT-PCRs were performed with 4 μg of total RNA of each set with M-MLV reverse transcriptase (Promega Corp. USA) and Taq polymerase (Sigma, USA) using primers designed from unique regions of *Eh Klp2–4*, *A1* and *Eh Actin* (endogenous control). To check the expression of Eh Klp2 and 5 in control, Eh Klp5 CHH and Eh Klp2 dsRNA transformants, semi-quantitative RT-PCRs were performed similarly with 4 μg of total RNA from each set using primers designed from unique regions of *Eh Klp2*, *5* and *Eh Actin*.

Quantitative PCR on cDNA from control and Eh Klp4 dsRNA transformants was carried out in a 7500 SDS Real-time instrument (Applied Biosystems, USA) using SYBR GREEN PCR Master Mix (Applied Biosystems, USA) according to the manufacturer's instructions. Specific primers to the unique region of *Eh Klp4* and *Eh Actin* were used for the PCR. All reactions were carried out in triplicate, and average threshold cycle values were calculated. Values of *Eh Klp4* were normalized with *Eh Actin* (endogenous control) and relative expression was calculated using the relative quantification software (Applied Biosystems, USA).

Cell lysis and Western analysis

Log-phase *E. histolytica* cells of control and Eh Klp transformants were lysed on ice in extraction buffer (10 mM Hepes-KOH, pH 7.2, 24 mM KCl, 10 mM $MgCl_2$) supplemented with 5% glycerol, complete protease inhibitor (Roche, Germany), 1 mM E-64 (Sigma, USA), 1 mM PMSF (Sigma, USA) and 1% Triton X-100. Total cellular proteins were measured using Bradford reagent (Bio-Rad, USA). Protein samples prepared from 40 μg of cell lysates were separated by SDS-PAGE and transferred to nitrocellulose membrane in three sets. The blots were hybridized with: (i) rabbit polyclonal Eh-Klp2 antibody (1:200 dilution); (ii) rabbit polyclonal Eh-Klp3 antibody (1:200 dilution); (iii) rabbit polyclonal Eh-KlpA1 antibody (1:200 dilution); (iv) rabbit polyclonal Eh β-tubulin antibody (1:500 dilution, Dastidar *et al*., 2007) and (v) mouse monoclonal anti-HA antibody 12CA5 (1:1000 dilution) respectively. This was followed by incubation with HRP-conjugated secondary antibodies (1:5000 dilution) and the signals were detected by chemi-luminescence using ECL kit (Roche, Germany). Eh Klp2 and 5 were detected similarly in control, Eh Klp5 CHH and Eh Klp2 dsRNA transformants.

Isolation of proteins bound to CHH-tagged Eh Klp2–5 and A1

The 48 h grown cells from control and Eh Klp transformants expressing CHH-tagged Eh Klp2–5, and A1 were sonicated in lysis buffer (20 mM Hepes-KOH, pH 7.4, 50 mM NaCl, 2 mM $MgCl_2$, 1 mM EGTA, 5% glycerol) supplemented with complete protease inhibitor mixture without EDTA (Roche, Germany), 1 mM E-64 (Sigma, USA) and 1 mM PMSF (Sigma, USA). The sonicated crude lysates were centrifuged at 13 000 *g* for 15 min at 4°C, and total protein was estimated in the supernatants using Bradford reagent (Bio-Rad, USA). About 2.5 mg of total proteins from each set was allowed to bind with Ni-NTA agarose beads in the presence of 10 μM taxol and 2 mM AMPPNP for 4 h at room temperature with constant agitation. The beads were centrifuged at 1000 *g* for 2 min and washed twice with lysis buffer alone and thrice with the lysis buffer supplemented with 30 mM imidazole. 2× SDS PAGE sample buffer was added to the beads and boiled

for 10 min. Protein samples were analysed by Western blotting followed by hybridization with rabbit polyclonal Eh Klp 2, 3, 5, and A1 antibodies (1:200 dilution), mouse monoclonal anti-HA (12CA5, Roche, Germany, 1:1000 dilution) and rabbit polyclonal Eh β-tubulin (1:500 dilution, Dastidar *et al*., 2007) overnight at 4°C. After hybridization with primary antibodies, the blots were incubated with HRP-conjugated secondary anti-mouse or anti-rabbit antibodies (1:5000, Sigma, USA) for 1 h at room temperature. The signals were detected by chemi-luminescence using ECL kit (Roche, Germany).

Isolation of actin-rich fraction

The actin-rich fractions were isolated from wild-type HM1:IMSS and Eh Klp4 CHH transformants, as described by Vargas *et al.* (1996). Forty micrograms of total proteins from the crude lysate and actin-rich fraction from wild-type cells was separated on SDS-PAGE and analysed by Western blot hybridization.

Immunofluorescence microscopy

Entamoeba histolytica trophozoites were allowed to grow on coverslips at 37°C and fixed directly on the coverslips with warm 3.7% formaldehyde for 15 min, washed with warm 1× PBS and permeabilized with 0.1% Triton X-100 for 10 min. Fixed cells were stained with anti-HA antibody, 12CA5 (1:200, Roche, Germany) and Alexa 488-conjugated anti-mouse secondary antibody (1:2500, Molecular probes, USA) to localize Eh Klps. This was followed by hybridization with specific antibodies as described in figure legends. Images were acquired either with a 40× oil objective (numerical aperture 1.3) in a Zeiss Axiovert 200 M fluorescence microscope using Z-stacking and deconvolution (Axiovision 3.1) or a 63× oil objective (numerical aperture 1.3) in a Zeiss LSM Meta confocal microscope equipped with 488 nm Argon laser and 543 nm He/Ne laser and analysed by LSM Meta software package.

Counting of cells with bipolar microtubular spindles

For determining bipolar spindle frequency, a total number of 300 fixed cells (three independent sets), stained with anti-Eh β-tubulin antibody were counted from each transformant under 40× objective of a Zeiss Axiovert 200 M fluorescence microscope using Axiovision 3.1 (Zeiss, Germany).

Analysis of DNA content by flow cytometry

To study the cellular DNA content, log-phase cells were harvested after 48 h of subculture and fixed in 70% ethanol at –20°C for 15 min. Fixed cells were washed in 1× PBS and treated with RNAse (0.3 mg ml^{-1},Sigma,USA) for at least 5 h and stained with propidium iodide (PI) (0.5 mg ml^{-1}, Sigma, USA) for 5 min in the dark. Flow cytometric analysis was carried out using FACSCalibur (Becton Dickinson, USA) equipped with a single-laser system (6 W Innova 90-6 argon ion laser). For measurement of DNA content, cells were excited with 488 nm light and emission was measured through 575DF20 (for PI fluorescence; FL2). Data from 10 000 cells were recorded for each experiment and analysed using Cellquest software (BD, USA).

Scanning cytometry to determine the DNA content of each nucleus

Cells were fixed with 70% ethanol and stained with DAPI (0.15 μg ml^{-1} for 5 min), washed twice with 1× PBS and spread evenly on glass slides. Each slide was scanned for DNA content of individual nuclei under 40× objective of a Zeiss Axiovert 200 M fluorescence microscope fitted with the MetaCyte scanning cytometer and Metafer4 software (Zeiss, Germany). A minimum of 2000 nuclei was scanned for each transformant. The DAPI fluorescence values were normalized for estimation of genome content and represented as histograms. Genome contents of transformants were normalized against control cells.

Sequence analysis of E. histolytica *kinesins*

Motor domains were identified from the amino acid sequences of *E. histolytica* kinesins with the help of Pfam and Conserved Domain Database searches in NCBI. Sequence alignments of Eh Klps and human conventional kinesin heavy chain was performed using ClustalW (Thompson *et al*., 1994) with BLOSUM62 matrix and default settings followed by manual editing with BioEdit software (URL: http://www.mbio.ncsu.edu/BioEdit/bioedit.html). Tools, such as SMART (URL: http://smart.embl-heidelberg.de/), TmPred (URL: http://www.ch.embnet.org/software/TMPRED_form.html) and 2Zip (URL: http://2zip.molgen.mpg.de/) were used to detect the presence of CC regions, TM helices and Leucine Zippers, respectively, in the Eh Klps.

Cloning, expression and purification of Eh Klp2–4 and A1 motor domain

The Eh Klp2 (1–347 aa), Eh Klp4 (1–329 aa) and Eh KlpA1 (1–335 aa) motor domains were cloned separately in the *E. coli* expression vector pQE30 and protein expression were induced using 400 μM IPTG in *E. coli* XL1-Blue transformants. Eh Klp3 motor domain (1–318 aa) was cloned in the *E. coli* expression vector pET28a and protein expression was induced with 500 μM IPTG in *E. coli* BL21 (DE3) transformants. 6× His-tagged recombinant Eh Klp2–4 and A1 motor domains were purified by Ni-NTA superflow matrix (Qiagen, Germany). The purified proteins were dialysed against ATPase assay buffer containing 5 mM $MgCl_2$, 1 mM EGTA, 1 mM DTT in 20 mM Tris-HCl (pH 7.5). ATPase activities of Eh Klp2–4 and A1 motor domains were assayed *in vitro* by a colorimetric method using Malachite green (Baykov *et al*., 1988).

Acknowledgements

This study was supported by NIH-sponsored FIRCA subgrants from University of Virginia (GC11289-123722; Primary award number 1RO3TW007314) and Stanford University (16846170-33918-A; Primary Award Number 1RO3TW007421-01), USA.

References

Baykov, A.A., Evtushenko, O.A., and Avaeva, S.M. (1988) A malachite green procedure for orthophosphate determination and its use in alkaline phosphatase-based enzyme immunoassay. *Anal Biochem* **171:** 266–270.

Blangy, A., Lane, H.A., d'Herin, P., Harper, M., Kress, M., and Nigg, E.A. (1995) Phosphorylation by p34cdc2 regulates spindle association of human Eg5, a kinesin-related motor essential for bipolar spindle formation *in vivo*. *Cell* **83:** 1159–1169.

Dagenbach, E.M., and Endow, S.A. (2004) A new kinesin tree. *J Cell Sci* **117:** 3–7.

Das, S., and Lohia, A. (2002) Delinking of S phase and Cytokinesis in the protozoan parasite *Entamoeba histolytica*. *Cellular Microbiol* **4:** 55–60.

Dastidar, P.G., Majumder, S., and Lohia, A. (2007) Eh Klp5 is a divergent member of the kinesin 5 family that regulates genome content and microtubular assembly in *Entamoeba histolytica*. *Cell Microbiol* **9:** 316–328.

Diamond, L.S., Harlow, D.R., and Cunnick, C.S. (1978) New medium for axenic cultivation of *Entamoeba histolytica* and other *Entamoeba*. *Trans R Soc Trop Med Hyg* **72:** 431–432.

Drummond, D.R., and Hagan, I.M. (1998) Mutations in the bimC box of Cut7 indicate divergence of regulation within the bimC family of kinesin related proteins. *J Cell Sci* **111:** 853–865.

Gangopadhyay, S.S., Ray, S.S., Kennady, K., Pande, G., and Lohia, A. (1997) Heterogeneity of DNA content in axenically growing *Entamoeba histolytica* HM1: IMSS clone A. *Mol Biochem Parasitol* **90:** 9–20.

Ghosh, S., Lohia, A., Kumar, A., and Samuelson, J. (1996) Overexpression of P-glycoprotein gene 1 by transfected *Entamoeba histolytica* confers emetine-resistance. *Mol Biochem Parasitol* **82:** 257–260.

Gordon, D.M., and Roof, D.M. (2001) Degradation of the kinesin Kip1p at anaphase onset is mediated by the anaphase-promoting complex and Cdc20p. *Proc Natl Acad Sci USA* **98:** 12515–12520.

Hildebrandt, E.R., and Hoyt, M.A. (2001) Cell cycle-dependent degradation of the *Saccharomyces cerevisiae* spindle motor Cin8p requires APC (Cdh1) and a bipartite destruction sequence. *Mol Biol Cell* **11:** 3402–3416.

Hildebrandt, E.R., Gheber, L., Kingsbury, T., and Hoyt, M.A. (2006) Homotetrameric form of Cin8p, a *Saccharomyces cerevisiae* kinesin-5 motor, is essential for its *in vivo* function. *J Biol Chem* **281:** 26004–26013.

Hirokawa, N., Noda, Y., and Okada, Y. (1998) Kinesin and dynein superfamily proteins in organelle transport and cell division. *Curr Opin Cell Biol* **10:** 60–73.

Honey, S., Schneider, B.L., Scieltz, D.M., Yates, J.R., and Futcher, B. (2001) A novel multiple affinity purification tag and its use in identification of proteins associated with a cyclin-CDK complex. *Nucleic Acid Res* **29:** E24.

Iwai, S., Ishiji, A., Mabuchi, I., and Sutoh, K. (2004) A novel actin-bundling kinesin-related protein from *Dictyostelium discoideum*. *J Biol Chem* **279:** 4696–4704.

Kim, A.J., and Endow, S.A. (2000) A kinesin family tree. *J Cell Sci* **113:** 3681–3682.

Kollmar, M., and Glöckner, G. (2003) Identification and phylogenetic analysis of *Dictyostelium discoideum* kinesin proteins. *BMC Genomics* **4:** 47.

Kull, F.J., Sablin, E.P., Lau, R., Fletterick, R.J., and Vale, R.D. (1996) Crystal structure of the kinesin motor domain reveals a structural similarity to myosin. *Nature* **380:** 550–555.

Kuriyama, R., Gustus, C., Terada, Y., Uetake, Y., and Matuliene, J. (2002) CHO1, a mammalian kinesin-like protein, interacts with F-actin and is involved in the terminal phase of cytokinesis. *J Cell Biol* **156:** 783–790.

Lohia, A., Mukherjee, C., Majumder, S., and Dastidar, P.G. (2007) Genome re-duplication and irregular segregation occur during the cell cycle of *Entamoeba histolytica*. *Biosci Rep* **27:** 373–384.

Miki, H., Okada, Y., and Hirokawa, N. (2005) Analysis of the kinesin superfamily: insights into structure and function. *Trends Cell Biol* **15:** 467–476.

Mountain, V., Simerly, C., Howard, L., Ando, A., Schatten, G., and Compton, D.A. (1999) The kinesin-related protein, HSET, opposes the activity of Eg5 and cross-links microtubules in the mammalian mitotic spindle. *J Cell Biol* **147:** 351–366.

O'Connell, M.J., Meluh, P.B., Rose, M.D., and Morris, N.R. (1993) Suppression of the bimC4 mitotic spindle defect by deletion of klpA, a gene encoding a KAR3-related kinesin-like protein in Aspergillus nidulans. *J Cell Biol* **120:** 153–162.

Ogawa, T., Nitta, R., Okada, Y., and Hirokawa, N. (2004) A common mechanism for microtubule destabilizers – M type kinesins stabilize curling of the protofilament using the class-specific neck and loops. *Cell* **116:** 591–602.

Orozco, E., Solis, F.J., Dominguez, J., Chavez, B., and Hernandez, F. (1988) *Entamoeba histolytica*: cell cycle and nuclear division. *Exp Parasitol* **67:** 85–95.

Preuss, M.L., Kovar, D.R., Lee, Y.R., Staiger, C.J., Delmer, D.P., and Liu, B. (2004) A plant-specific kinesin binds to actin microfilaments and interacts with cortical microtubules in cotton fibers. *Plant Physiol* **136:** 3945–3955.

Richardson, D.N., Simmons, M.P., and Reddy, A. (2006) Comprehensive comparative analysis of kinesins in photosynthetic Eukaryotes. *BMC Genomics* **7:** 18.

Sablin, E.P., Kull, F.J., Cooke, R., Vale, R.D., and Fletterick, R.J. (1996) Crystal structure of the motor domain of the kinesin-related motor ncd. *Nature* **380:** 555–559.

Sawin, K.E., and Mitchison, T.J. (1995) Mutations in the kinesin-like protein Eg5 disrupting localization to the mitotic spindle. *Proc Natl Acad Sci USA* **92:** 4289–4293.

Sharp, D.J., Rogers, G.C., and Scholey, J.M. (2000) Microtubule motors in mitosis. *Nature* **407:** 41–47.

Thompson, J.D., Higgins, D.G., and Gibson, T.J. (1994) CLUSTAL W: improving the sensitivity of progressive multiple sequence alignment through sequence weighing, position-specific gap penalties and weight matrix choice. *Nucleic Acids Res* **22:** 4673–4680.

Vargas, M., Sansonetti, P., and Guillen, N. (1996) Identification and cellular localization of the actin-binding protein ABP-120 from *Entamoeba histolytica*. *Mol Microbiol* **22:** 849–857.

Vayssie, L., Vargas, M., Weber, C., and Guillen, N. (2004) Double-stranded RNA mediated homology-dependent gene silencing of gamma tubulin in the human parasite *Entamoeba histolytica*. *Mol Biochem Parasitol* **138:** 21–28.

Wickstead, B., and Gull, K. (2006) A 'holistic' kinesin phylogeny reveals new kinesin families and predicts protein functions. *Mol Biol Cell* **17:** 1734–1743.

Wittman, T., Hyman, A., and Desai, A. (2001) The spindle: a dynamic assembly of microtubules and motors. *Nature Cell Biol* **3:** E28–E34.

Supplementary material

The following supplementary material is available for this article online:

Fig. S1. *In vitro* ATPase activities of Eh Klp2–4 and A1 motor domain. *In vitro* ATPase activities of purified Eh Klp2–4 and A1 motor domains were measured using Malachite green method. 2 μM of each of the purified proteins were incubated with 100 μM ATP as the substrate. The increase of released Pi was measured as a function of time. Error bars indicate ± SD ($n = 3$).

Fig. S2. Localization of CHH epitope-tagged Eh Klp2–3, 5 and A1 with endogenous Eh Klps in stable transformants. Trophozoites were grown on coverslips at 37°C and fixed directly. CHH epitope-tagged Eh Klp2, 3, 5 and A1 transformants were stained (a) with mouse monoclonal anti-HA antibody to detect the epitope tagged Eh Klps (HA) and (b) with specific anti-Eh Klp rabbit polyclonal antibodies to detect endogenous and tagged Eh Klps (Eh Klp2, 3, 5, A1). Cells were visualized under 63× oil, DIC objective in a Zeiss LSM 510 Meta confocal microscope. Bar represents 5 μm.

Fig. S3. A. Immuno-localization of Eh Klp 2, 3, A1 in wild-type *E. histolytica* HM1:IMSS and dsRNA transformants Eh Klp2, 3 and A1 were localized with specific anti-Eh Klp polyclonal antibodies in the respective dsRNA transformants and wild-type cells. The corresponding DIC images were shown in each panel. Cells were visualized under 63× oil, DIC objective in a Zeiss LSM 510 Meta confocal microscope. Bar represents 5 μm.

B. Microtubular assemblies in control and Eh Klp2–4 and A1 dsRNA transformants. Trophozoites were grown on coverslips at 37°C and fixed directly. Both bipolar spindle (white arrows with filled arrowheads) and radial microtubular assemblies (white arrows) were stained with anti-Eh β tubulin polyclonal antibody in control, Eh Klp2–4 and A1 dsRNA transformants. DNA was stained with DAPI. Cells were visualized under 40× oil objective in a Zeiss Axiovert 200 M fluorescence microscope. Bar represents 5 μm.

Fig. S4. Changes in expression levels of Eh Klp3, 4 and A1 shows no effect on the genome content of *E. histolytica*.

A. 48 h grown cells of control, CHH-tagged and dsRNA transformants of Eh Klp3, 4 and A1, maintained with 40 μg ml^{-1} concentration of G418, were fixed and stained with PI to analyse the average DNA content. Representative histograms obtained from the flow cytometric analyses of Eh Klp3, 4 and A1 transformants with control cells were shown as overlay diagrams.

B. The DNA content of individual nuclei from DAPI-stained cells of control, CHH-tagged and dsRNA transformants of Eh Klp3, 4 and A1, maintained at 40 μg ml^{-1} concentration of G418, were determined in a Metacyte scanning cytometer using Metafer4 software. A minimum of 2000 nuclei was scanned for each set. DAPI fluorescence values for each nucleus from Eh Klp3, 4 and A1 transformants were normalized with respect to the control transformant and represented as histograms.

This material is available as part of the online article from:
http://www.blackwell-synergy.com/doi/abs/10.1111/j.1462-5822.2008.01150.x

Please note: Blackwell Publishing is not responsible for the content or functionality of any supplementary materials supplied by the authors. Any queries (other than missing material) should be directed to the corresponding author for the article.

